



APPLICATION OF ARTIFICIAL NEURAL NETWORK IN PREDICTING THE DRYING KINETICS AND CHEMICAL ATTRIBUTES OF LINDEN (*TILIA PLATYPHYLLOS* SCOP.) DURING THE INFRA-RED DRYING PROCESS

Kemal Çağatay SELVI¹, Alfadhil Yahya KHALED², Taner YILDIZ¹

¹Department of Agricultural Machinery and Technologies Engineering, Faculty of Agriculture, University of Ondokuz Mayıs-Samsun/Turkey

²Department of Horticulture, College of Agricultural & Life Sciences, University of Wisconsin – Madison, Madison, WI, USA

Abstract

This study investigates the potential of applying artificial neural networks (ANNs) to describe the drying kinetics of linden leaf samples during infra-red drying (IRD) under different drying temperatures of 50°C, 60°C and 70°C and samples thickness (0.210, 0.220, and 0.230). Kinetic models were developed using selected thin layer models, and ANN methods. The statistical indicators of the coefficient of determination (R^2), and root mean square error (RMSE) were used to evaluate the suitability of the models. The effective moisture diffusivity varied between $4.13 \times 10^{-12} \text{ m}^2/\text{s}$ and $5.89 \times 10^{-12} \text{ m}^2/\text{s}$ and the activation energy was 16.339 kJ/mol. The thin-layer models illustrated that all used models (Page, Midilli et al., Henderson and Pabis, Logarithmic, and Newton models) can adequately describe the drying kinetics of linden leaf samples with R^2 values (> 0.9900) and lowest RMSE (< 0.0200). The ANN model showed R^2 and RMSE values of 0.9986, and 0.0210, respectively. Also, the ANN model shows the significant prediction for the linden chemical attributes for Total phenolics content (TPC), Total flavonoids assay (TFA), DPPH, and FRAP of R^2 and RMSE values of 0.9975, 2.6100, 0.9891, 0.1346, 0.9980, 2.9317, 0.9845, and 0.9808, respectively.

Key words: linden leaves, infrared drying, artificial neural network model; total phenolic content; total flavonoid, DPPH, FRAP content.

INTRODUCTION

Linden (*Tilia platyphyllos* Scop.) is a medicinal plant with a pleasant taste in its tea which has several dozen different species and varieties (Chmielewska & Sadowska, 2010). It is rich in polyphenols and presents high antioxidant activity against DPPH radicals (Wissam, Nour, Bushra, Zein & Saleh, 2017; Siger, Antkowiak, Dwiecki, Rokosik & Rudzińska, 2021). The high agricultural value of linden in terms of many valuable elements it contains is emphasized in many articles (Yıldırım, Mavi, Oktay, Kara, Algur & Bilaloğlu, 2000; Buřičová & Reblova 2008; Kowalski 2017; Kelmendi, Mustafa, Zahiri, Nebija & Hajdari, 2020).

The drying of agricultural products causes the enzymatic reactions to be inactivated as a result of heat and mass transfer leading to a reduction of the moisture content inside the product (Rodríguez, Clemente, Sanjuan & Bon, 2013). Drying methods such as hot-air drying (HAD), infrared drying (IRD), vacuum drying (VD), and microwave drying (MWD) have been used in drying agricultural crops (Onwude, Hashim, Abdan, Janius & Chen, 2018; Si, Wu, Yi, Li, Chen, Bi & Zhou, 2015; Tekin & Baslar, 2018). Amongst these drying methods, the IRD is the most common commercially used drying method as they provide a more uniform dried product, naturally harmless and nontoxic (Onwude, Hashim, Janius, Nawi & Abdan, 2016).

IRD radiation had been implemented in food processing, reducing energy consumption and time spent in the process, securing and ensuring the quality of foodstuffs processed. There are some studies, related to the IRD process, reported in the literature on mint (Ertekin & Heybeli, 2014), pepper (Soysal, Keskin, Arslan & Sekerli, 2018), and kiwifruit slices (Doymaz, 2018). Computational intelligence tools such as artificial neural networks (ANN) are considered complex tools for complex systems and dynamic modeling (Khaled, Aziz, Bejo, Nawi & Abu Seman, 2018). The application of ANN offers many advantages compared to conventional modeling techniques due to the learning ability, improved flexibility, online non-destructive measurements, reduced assumptions, suitability to the non-linear process, and tolerance



of incomplete data (Bai *et al.*, 2018). For instance, ANN is inspired by the biological neural system as a useful statistical tool for nonparametric regression (Khaled, Aziz, Bejo, Nawi & Abu Seman, 2018). The objectives of this study are to investigate the drying characteristics of linden leaf samples at different temperatures (50°C, 60°C, and 70°C) using IRD, to evaluate the likelihood of applying ANN modeling as a non-destructive technique in describing the drying behavior of linden leaf samples under different drying conditions and to compare the results with mathematical thin-layer models.

MATERIALS AND METHODS

Samples preparation

Linden leaves (*T. platyphyllos* Scop.) were collected from the campus area of Ondokuz Mayıs University under open-air conditions located in the Samsun city coastline, Black Sea region, Turkey.

Drying experiments

The IRD technique was carried out using a laboratory-scale drying unit (Radweg balances and scales, Warsaw, Poland). This device has transmitting electromagnetic radiation in the range of medium to shortwave IR (radiator). The linden leaf samples were dried at three temperatures (50°C, 60°C, and 70°C). During drying, the amount of evaporating water was designated in about 3-min intervals at each drying temperature. Trials were replicated three times and average weight loss was reported.

Drying kinetics

The variation in moisture content during the IRD technique was expressed in the form of moisture ratio (dimensionless) as described in Equation 1.

$$MR = \frac{(M_t - M_e)}{(M_o - M_e)} \quad (1)$$

where M_t , M_e and M_o are the moisture content of the samples at time t , equilibrium moisture content and initial moisture content, respectively. According to Aghbashlo *et al.* (2009) M_e values did not change because they were relatively low compared to M_t and M_o values, resulting in negligible error during simplification, thus in this study, the moisture ratio was expressed as shown in Equation 2:

$$MR = \frac{M_t}{M_o} \quad (2)$$

Effective moisture diffusivity and activation energy

Fick's diffusion equation as a dimensional approach was applied due to its simplicity to describe the mass transfer of drying samples. The effective moisture diffusivity of samples for IRD was estimated using Crank's solution of Fick's diffusion equation as described in Equation 3 (Erbay and Icier, 2010).

$$\frac{\partial M_t}{\partial t} = \nabla \cdot (D_{eff} \nabla M_t) \quad (3)$$

Assuming constant diffusion and uniform initial moisture distribution, the Crank's solution for cylindrical shaped sample is shown in Equation 4.

$$MR = \frac{8}{\pi^2} \sum_{n=1}^{\infty} \frac{1}{(2n+1)^2} \exp\left(-\frac{(2n+1)^2 D_{eff} t}{r^2}\right) \quad (4)$$

where D_{eff} is the effective moisture diffusivity (m^2/s), r is the radius of the sample (m), n is the positive integer, and t is the drying time (s). For the sake of mathematical simplicity, Equation 4 was restricted to the first term, resulting in Equation 5:

$$MR = \frac{8}{\pi^2} \exp\left(-\frac{\pi^2 D_{eff} t}{r^2}\right) \quad (5)$$

The activation energies for IRD were calculated from the relationship between effective moisture diffusivity and the average temperature of the samples based on the Arrhenius equation as shown in equation (6).

$$D_{eff} = D_o \exp\left(-\frac{E_a}{R(T + 273.15)}\right) \quad (6)$$

where, D_o is the pre-exponential factor, E_a is the activation energy (kJ/mol), R is the universal gas constant ($8.3143 \times 10^{-3} kJ/mol$) and T is the average temperature of the sample (K). The values of E_a for



IRD method for different linden leaf thickness levels were measured from the resulting slope values by plotting the fitting curve between $\ln D$ and $1/(T + 273.15)$ (Equation 7).

$$\text{Slope} = - \frac{E_a}{R} \quad (7)$$

Mathematical thin-layer modelling

The selected mathematical models namely: Page, Midilli et al., Henderson and Pabis, Logarithmic, and Newton model as listed in Table 1. The mathematical models applied based on non-linear least squares regression analysis using Sigma plot software (Version 12.0, Systat Software Inc., California, USA). The application of these models gives better prediction with fewer assumptions (Khaled, Kabutey, Selvi, Mizera, Hrabe & Herak, 2020).

Tab. 1 Mathematical thin-layer drying models.

Model no.	Model name	Model expression
1.	Page model	$MR = \exp(-ktn)$
2.	Midilli et al. model	$MR = a \exp(-kt) + bt$
3.	Henderson and Pabis model	$MR = a \exp(-kt)$
4.	Logarithmic model	$MR = a \exp(-kt) + c$
5.	Newton model	$MR = \exp(-kt)$

Artificial neural network

The structure of a neural network is in the form of interconnected layers. Haykin (1999) divided an ANN into 3 clusters of structures based on their connection called: (1) single layer feed-forward network, (2) the multi-layer feed-forward network, and (3) the recurrent network. A back-propagation algorithm was applied in the training of the model and sigmoid function was used in all cases as illustrated in Equation 8.

$$f(x) = \frac{1}{1 + e^{-x}} \quad (8)$$

The datasets were prepared by randomly dividing the data into training and testing datasets of 70%, 30%, respectively. The chosen hidden layer architectures were [3], [6], [9], [3, 3], [6, 6], [9, 9], [3, 3, 3], [6, 6, 6] and [9, 9, 9] matrix, where for example, [3, 3] and [3, 3, 3], represents the 2 and 3 hidden layers with 6 and 9 neurons each (Figure 1). The software (Weka 3.6, Hamilton, New Zealand) was used to analyze the ANN model.

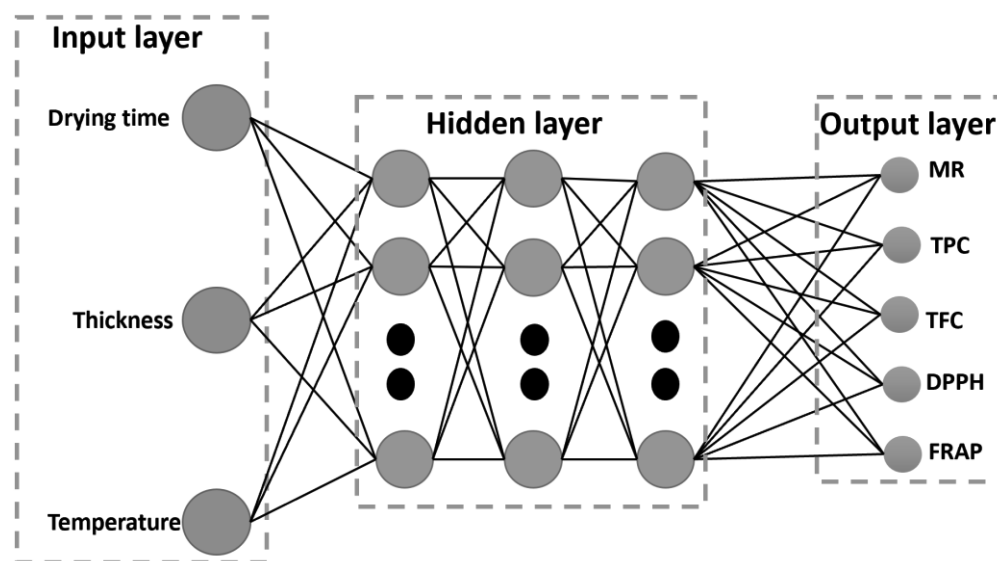


Fig. 1 Artificial Neural networks topology applied for this study



Extract preparation of the chemical characteristics

The powdered sample was extracted with methanol/distilled water (80:20, v/v) for 12 hours at room temperature by the maceration method, and centrifuged for 20 min. The supernatant was used for the estimation of antioxidants and antioxidant activity. The total phenolic content (TPC) was determined by applying the Folin-Ciocalteu method (*Singleton and Rossi, 1965*). For the total flavonoids content (TFC) was measured using an AlCl₃ colorimetric assay according to *Gao et al. (2014)*.

Free radical scavenging activity was measured using the stable DPPH free radical, according to the method described by *Brand-Williams et al. (1995)*. The scavenging activity on the DPPH free radical was compared with that of the Trolox, a water-soluble vitamin E analog. Results were expressed in mmol Trolox equivalents (TE)/g of powder. The ferric reducing/antioxidant power (FRAP) assay was conducted according to *Benzie and Strain (1996)*.

Statistical analysis for mean comparison

Statistical analysis was performed using the Statistical Analysis System software (SAS version 9.2, Institute, Inc., Cary, N.C.). ANOVA at 5% level of significance and 95% confidence interval was performed using the Duncan test to compare the mean significant differences between different drying time intervals at the IRD technique. These statistical indicators are the coefficient of determination (R²) and root mean square error (RMSE). They are computed mathematically as highlighted in Equations 9 and 10:

$$R^2 = 1 - \frac{\sum_{i=1}^N (V_{pred} - V_{exp})^2}{\sum_{i=1}^N (V_{pred} - V_m)^2} \quad (9)$$

$$RMSE = \sqrt{\frac{\sum_{i=1}^N (V_{pred} - V_{exp})^2}{N}} \quad (10)$$

where V_{pred} is the predicted value, V_{exp} is the actual observation from experimental data, V_m is the mean of the actual observation, and N is number of observations.

RESULTS AND DISCUSSION

Drying process behavior

The variations of moisture ratio with time for the IRD technique at different temperatures (50°C, 60°C, and 70°C) is presented in Figure 2. According to Figure 2, the moisture ratio values of 0.20 and 0.42 were determined at a drying time of 10 min and at temperatures of 60°C and 70°C. At a drying time of 37 min was found the moisture ratio of 0.20 at 50°C. Also, results showed that higher drying temperature resulted in a greater slope and the drying time is reduced by about 250%. The results are in agreement with other researchers on the drying behavior of various varieties of materials (*Ayadi, Ben Mabrouk, Zouari, Bellagi, 2014; Khaled, Kabutey, Selvi, Mizera, Hrabe & Herak, 2020*).

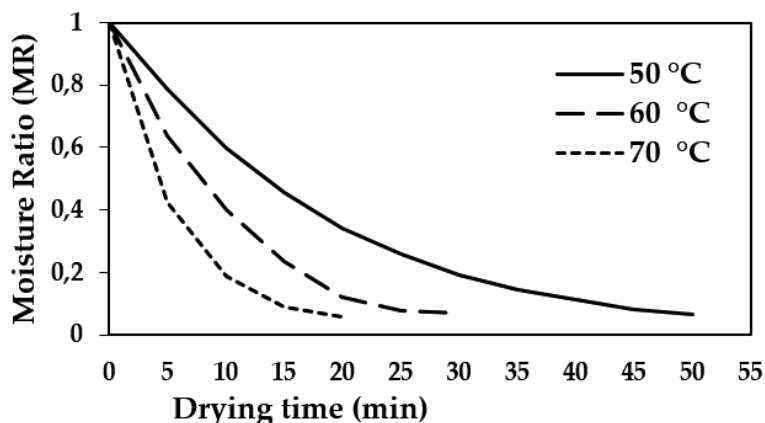


Fig. 2 Drying characteristics of linden leaf samples



Effective moisture diffusivity and activation energy

The values of the D_{eff} are presented in Table 2. The D_{eff} values were varied between the range of $4.13 \times 10^{-12} \text{ m}^2/\text{s}$ and $5.89 \times 10^{-12} \text{ m}^2/\text{s}$. The values of D_{eff} obtained in this study were within the general range of 10^{-6} to $10^{-12} \text{ m}^2/\text{s}$ for drying of food materials. The values of D_{eff} are comparable with previous works for strawberry drying ($2.40\text{-}12.1 \times 10^{-9} \text{ m}^2/\text{s}$), apple drying ($2.27\text{-}4.97 \times 10^{-10} \text{ m}^2/\text{s}$), persimmon slices ($1.330\text{-}9.221 \times 10^{-9} \text{ m}^2/\text{s}$) and pumpkin drying ($1.19\text{-}4.27 \times 10^{-9} \text{ m}^2/\text{s}$) (Xiao, Pang, Wang, Bai, Yang & Gao, 2010; Abbaspour-Gilandeh, Jahanbakhshi & Kaveh, 2020; Sacilik & Elicin, 2006). On the other hand, the diffusivity constant in other words “pre-exponential factor” of the Arrhenius equation (D_0) was predicted as $1.746 \times 10^{-9} \text{ m}^2/\text{s}$ for linden leaves. The activation energy (E_a) of linden leave samples was calculated from the values of effective moisture diffusivity. The relationship between E_a and D_{eff} was described by an Arrhenius-type equation (Equation 6). The values of activation energy were obtained by plotting $\ln(D_{eff})$ versus $1/(T+273.15)$ for the IRD method (Figure 3).

Tab. 2 Values for D_{eff} and E_a of linden leave samples during IRD technique.

Drying Temperature (°C)	D_{eff} (m ² /s)	D_0 (m ² /s)	E_a (kJ/mol)
50	4.13×10^{-12}	1.746×10^{-9}	16.339
60	4.47×10^{-12}		
70	5.89×10^{-12}		

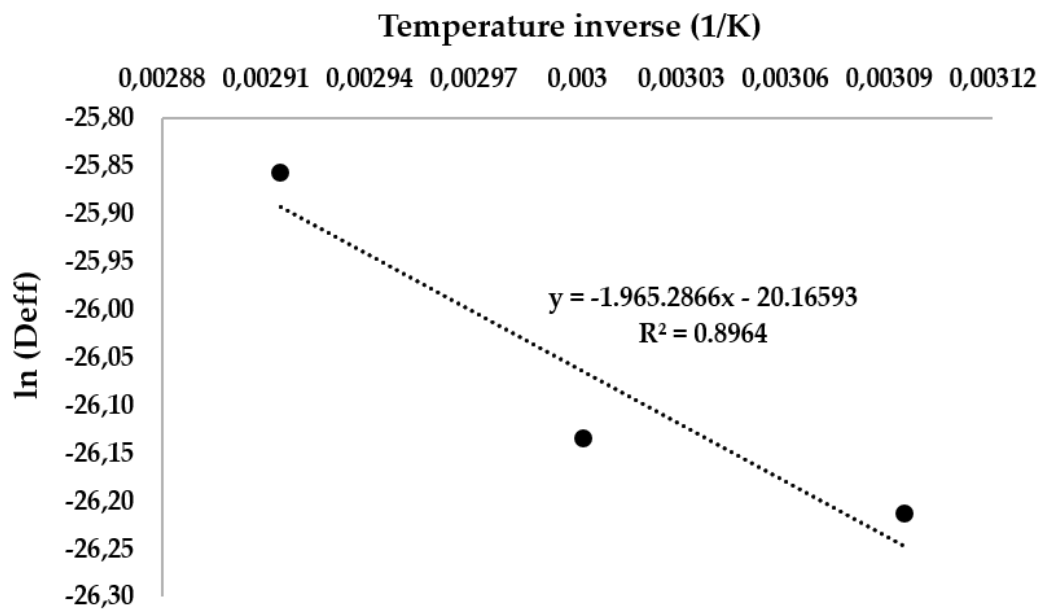


Fig. 3 Arrhenius-type relationship of E_a versus temperature for IRD method

A Comparison between mathematical thin-layer models

The mathematical thin-layer models were applied to describe the drying kinetics of linden leave samples during the IRD method. Table 3 shows the selected mathematical models that fitted the experimental moisture content data in relation to the sample.

Tab. 3 Statistical evaluation of the mathematical drying models for linden leaves samples of IRD

Drying Temperature (°C)	Model no	Model parameters	R ²	RMSE
50	1	k= 0.0472, n= 1.0381,	0.9992	0.0090
	2	k= 0.0413, n= 1.0933, a= 0.9998, b= 0.0003	0.9999	0.0025
	3	a= 1.0128, k= 0.0538	0.9990	0.0098



60	4	a= 1.0096, k= 0.0547, c= 0.0053	0.9991	0.0099
	5	k= 0.0532	0.9988	0.0104
	1	k= 0.0955, n= 0.9915	0.9935	0.0257
	2	k= 0.0716, n= 1.1305, a= 0.9984, b= 0.0009	0.9992	0.0102
	3	a= 1.0032, k= 0.0937	0.9935	0.0256
70	4	a= 0.9844, k= 0.1028, c= 0.0286	0.9969	0.0188
	5	k= 0.0934	0.9935	0.0245
	1	k= 0.2584, n= 0.7815	0.9931	0.0269
	2	k= 0.1300, n= 1.1340, a= 0.9914, b= 0.0013	0.9984	0.0152
	3	a= 0.9935, k= 0.1625	0.9896	0.0330
	4	a= 0.9611, k= 0.1866, c= 0.0405	0.9998	0.0055
	5	k= 0.1635	0.9896	0.0312

Results of artificial neural network

Time, temperature, and linden leaf thickness levels were used to predict moisture ratio using the ANN model at IRD technique. Tables 4 show the statistical results related to training and validation of the multilayer feed-forward network structure of samples drying experimental data for the IRD method.

Tab. 4 Statistical results of drying kinetics of linden leaves samp. for the ANN model using IRD

No. hidden layer	No. Neurons	Training		Testing	
		R ²	RMSE	R ²	RMSE
1	3	0.9620	0.0654	0.9978	0.0152
1	6	0.9602	0.0666	0.9943	0.0194
1	9	0.9717	0.0566	0.9866	0.0302
2	3,3	0.9549	0.0706	0.9974	0.0132
2	6,6	0.9769	0.0546	0.9986	0.0210
2	9,9	0.9743	0.0568	0.9974	0.0327
3	3,3,3	0.9424	0.0795	0.9962	0.0215
3	6,6,6	0.9672	0.0616	0.9971	0.0163
3	9,9,9	0.9704	0.0587	0.9961	0.0412

Comparison between artificial neuron networks and mathematical thin-layer models

The highest results obtained from the computational intelligence (ANN) and the top two mathematical thin-layer (page, Midilli et al, and Logarithmic) models of prediction moisture ratio is summarized in Table 5. The best results found by applying ANN in the case of IRD method were R² of 0.9986 and RMSE of 0.0210 at 2 hidden layers with 12 neurons.

Tab. 5 Statistical results of drying kinetics of linden leaf samples for artificial neural networks and mathematical thin-layer models using IRD

Model		R ²	RMSE
Computational intelligence	ANN	0.9986	0.0210
Mathematical model	Logarithmic	0.9998	0.0055
	differences	0.9992	0.0090
	Midilli et al.	0.9999	0.0025



Total Phenolic Content (TPC) and Flavonoids (TFC)

The results are given by calculating dry matter values to prevent errors arising from dry matter difference. The total phenolic content (TPC) of fresh leaves material was significantly ($p < 0.05$) higher than dried leaves. Table 6 presents the TPC and TFC content of the linden leaves under different temperatures process.

Tab. 6 Total phenolic and flavonoid content of the fresh and dried linden leaves.

Temperature (°C)	TPC (mg/g, DW)	TFC (mg/g, DW)
Fresh	12.773 ± 0.76 b	0.567 ± 0.015 b
50	95.184 ± 0.47 a	2.790 ± 0.150 a
60	99.756 ± 0.63 a	2.631 ± 0.084 a
70	99.756 ± 0.63 a	2.583 ± 0.145 a
Significance	<0.001	<0.001

The total phenolic content (TPC), total flavonoid content (TFC), a, b: Different letters within same column shows the statistical difference ($p < 0.01$).

To analyze the data, a non-parametric permutation test was used because of heteroscedasticity. TPC and TFC values were corrected and evaluated based on dry matter values to prevent errors arising from dry matter differences. Table 6 shows that the TPC of linden leaves was significantly different between fresh and dried samples and the values ranged from 99.756 ± 0.63 mg/g to 127.73 ± 0.76 mg/g. The TPC in the dried leaves (for 50 °C, 60 °C, 70 °C) was significantly ($p < 0.001$) lower than that in the fresh.

On the other hand, as can be seen in Table 6, the Duncan test indicates no statistical difference among temperatures (50 °C, 60 °C, and 70 °C). This means that linden leaves seem to be thermostable in the studied temperature range.

The TFC in linden leaves is shown in Table 5; it varied significantly between fresh and dried samples and ranged from 0.567 ± 0.015 mg/g to 2.790 ± 0.150 mg/g. The reason for this may be the decrease of the solution viscosity due to the increase in temperature as the lime leaves change from a wet state to a dry state, and the increase of solubility, accordingly. In this study, depending on the type of flavonoids and the number of substituents, there could be no change in the flavonoid contents. In addition, the TFC results obtained in the present study correlated with Olsson et al.

This finding suggests that besides the Midilli drying model, a simpler Page model can also be preferred for linden leaves under an IR thin layer drying process. In addition, 50 °C will be sufficient in terms of phenol content and flavonoid content in a thin layer lime leaf drying process with IR.

Results of artificial neuron networks to predict chemical properties of linden leave samples

Temperature and linden leaf thickness levels were used to predict total phenolics (mg/g, DW), Total flavonoids (mg/g, DW), DPPH (mmol/g, DW), and FRAP (mmol/g, DW) using ANN model. Tables 7 illustrate the statistical results from the four chemical properties of the multilayer feed-forward network structure of samples drying experimental data. The ANN data set were used to assess the optimum number of neurons and hidden layers for multilayer neural network modelling for determining the best predictive power. In the case of total phenolics, total flavonoids, and FRAP, the results found that architecture with 2 hidden layers with 6 (3, 3 neurons), obtained the best results of R^2 (0.9975, 0.9891, and 0.9845) and the lowest RMSR of (2.6100, 0.1346, and 0.9808) as compared to those of 1 hidden layer (3, 6 and 9 neurons), 2 hidden layers (12, 18 neurons) and 3 hidden layers (9, 18 and 27 neurons), respectively (Table 6). While, DPPH, the highest results were found that architecture with 3 hidden layers with 18 (6, 6, 6 neurons), obtained the best results of R^2 (0.9980) and the lowest RMSR of (2.9317) as compared to those of 1 hidden layer (3, 6 and 9 neurons), 2 hidden layers (6, 12, 18 neurons) and 3 hidden layers (9 and 27 neurons), respectively (Table 7).

**Tab. 7** Statistical results of chemical characteristics of linden leave for the ANN model using IRD.

No. Hidden Layer	No. Neurons	Total phenolics (mg/g, DW)		Total flavonoids (mg/g, DW)		DPPH, mmol/g, DW		FRAP, mmol/g, DW	
		R ²	RMSE	R ²	RMSE	R ²	RMSE	R ²	RMSE
1	3	0.9969	2.8914	0.9884	0.1393	0.9977	3.1420	0.9816	1.0760
1	6	0.9965	3.1026	0.9882	0.1404	0.9977	3.1396	0.9824	1.0485
1	9	0.9965	3.0855	0.9877	0.1439	0.9975	3.3549	0.9839	1.0017
2	3,3	0.9975	2.6100	0.9891	0.1346	0.9978	3.0660	0.9845	0.9808
2	6,6	0.9974	2.6835	0.9890	0.1356	0.9978	3.0664	0.9840	0.9986
2	9,9	0.9972	2.7533	0.9888	0.1370	0.9978	3.0894	0.9833	1.0197
3	3,3,3	0.9970	2.8433	0.9881	0.1401	0.9979	3.0421	0.9826	1.0402
3	6,6,6	0.9968	2.9741	0.9876	0.1439	0.9980	2.9317	0.9818	1.0690
3	9,9,9	0.9965	3.0873	0.9873	0.1460	0.9979	3.0024	0.9812	1.0906

CONCLUSIONS

This study investigated the potential of using the ANN as a modeling tool for predicting the drying process and the chemical characteristics of linden leave samples. The results showed that IRD had a significant effect on the drying kinetics, moisture diffusivity, and activation energy of linden leave samples. An increase in drying temperature and sample thickness influenced the drying kinetics and moisture diffusivity of samples. The effective moisture diffusivity varied between $4.13 \times 10^{-12} \text{ m}^2/\text{s}$ and $5.89 \times 10^{-12} \text{ m}^2/\text{s}$ and the activation energy was 16.339 kJ/mol. The mathematical thin-layer modeling results showed that page, Midilli et al., and Logarithmic models can adequately ($R^2 > 0.9900$) describe the drying kinetics of linden leave samples. The highest R^2 value of 0.9986 was observed for ANN (2 hidden layers with (6, 6) neurons) model. ANN tool as a computational intelligence method produced closer results compared to mathematical thin-layer. Also, the ANN model shows the significant prediction for the linden chemical attributes for Total phenolics content (TPC), Total flavonoids assay (TFA), DPPH, and FRAP of R^2 and RMSE values of 0.9975, 2.6100, 0.9891, 0.1346, 0.9980, 2.9317, 0.9845, and 0.9808, respectively. Therefore, the ANN model can describe a wider range of experimental data whereas the application of theoretical models is limited to specific experimental conditions in most cases. Thus, ANN may be considered a suitable alternative modeling method for describing the drying behavior of linden leave samples.

A universal method for appropriate estimation of wire diameter of helical compression spring was determined. The estimation can be based only on the amount and type of load and selected wire material. This procedure can be useful when only force and deflection of spring are specified.

REFERENCES

1. Abbaspour-Gilandeh, Y., Jahanbakhshi, A., & Kaveh, M. (2020). Prediction kinetic, energy and exergy of quince under hot air dryer using ANNs and ANFIS. *J. Sci. Food Agric.*, 8, 594–611.
2. Aghbashlo, M., Kianmehr, M.H., Khani, S., & Ghasemi, M. (2009). Mathematical modelling of thin-layer drying of carrot. *Int. Agrophys.*, 23, 313–317.
3. Ayadi, M. Ben Mabrouk, S., Zouari, I., & Bellagi, A. (2014). Kinetic study of the convective drying of spearmint. *J. Saudi Soc. Agric. Sci.*, 13, 1–7.
4. Bai, J., Xiao, H., Ma, H. & Zhou, C. (2018). Artificial neural network modeling of drying kinetics and color changes of ginkgo biloba seeds during microwave drying process. *J. Food Qual.*, 1–8.
5. Benzie, IFF. & Strain, JJ. (1996). The Ferric Reducing ability of plasma (FRAP) as a measure of Antioxidant power: The FRAP assay. *Analytical Biochemistry*, 239 (1),70-76.
6. Brand-Williams, W., Cuvelier., M.E. & Berset, C. (1995). Use of a free radical method to evaluate antioxidant activity. *LWT*, 28:25-30.
7. Buřičová, L. & Reblova, Z. (2008). Czech medicinal plants as possible sources of antioxidants. *Czech J. Food Sci*, 26(2), 132-138.



8. Doymaz, I. (2018). Infrared drying of kiwifruit slices. *Int. J. Green Energy*, 15, 622–628.
9. Erbay, Z. & İcier, F. (2010). A Review of Thin Layer Drying of Foods: Theory, Modeling, and Experimental Results. *Crit Rev Food Sci Nutr*. 50 (5). 441-464.
10. Ertekin, C. & Heybeli, N. (2014). Thin-layer infrared drying of mint leaves. *J. Food Process. Preserv.* 38, 1480–1490.
11. Gao, H., Cheng, N., Zhou, J., Wang, B.N., Deng, J.J. & Cao, W. (2014). Antioxidant activities and phenolic compounds of date plum persimmon (*Diospyros lotus* L.) fruits. *J Food Sci Technol.*, 51(5):950-956.
12. Haykin, S. (1999). Neural Networks a Comprehensive Introduction; *Prentice Hall: Upper Saddle River, NJ, USA*,
13. Kelmendi, N., Mustafa, B., Zahiri, F., Nebija, D., & Hajdari, A. (2020). Essential Oil Composition of *Tilia platyphyllos* Scop. Collected from Different Regions of Kosovo. *Records of Natural Products*, 14(5), 371.
14. Khaled, A.Y., Aziz, S.A., Bejo, S.K., Nawi, N.M., & Abu Seman, I.A. (2018). Spectral features selection and classification of oil palm leaves infected by Basal stem rot (BSR) disease using dielectric spectroscopy. *Comput. Electron. Agric.*, 144, 297–309.
15. Khaled, A.Y.; Kabutey, A.; Selvi, K.Ç.; Mizera, C.; Hrabe, P. & Herak, D. (2020). Application of computational intelligence in describing the drying kinetics of persimmon fruit (*Diospyros kaki*) during vacuum and hot air drying process. *Processes*, 8(5), 544.
16. Kowalski, R., Baj, T., Kalwa, K., Kowalska, G., & Sujka, M. (2017). Essential oil composition of *Tilia cordata* flowers. *Journal of Essential Oil Bearing Plants*, 20(4), 1137-1142.
17. Olsson, M.E., Gustavsson, K.E. & Vågen, I.M. (2010). Quercetin and isorhamnetin in sweet and red cultivars of onion (*Allium cepa* L.) At harvest, after field curing, heat treatment, and storage. *J. Agric. Food Chem.* 58(4), 2323–2330.
18. Onwude, D., Hashim, N., Abdan, K., Janius, R. & Chen, G. (2018). The potential of computer vision, optical backscattering parameters and artificial neural network modelling in monitoring the shrinkage of sweet potato (*Ipomoea batatas* L.) during drying. *J. Sci. Food Agric.*, 98, 1310–1324.
19. Onwude, D.I., Hashim, N., Janius, R.B., Nawi, N. & Abdan, K. (2016). Evaluation of a suitable thin layer model for drying of pumpkin under forced air convection. *Int. Food Res. J.*, 23, 1173
20. Rodríguez, J., Clemente, G., Sanjuan, N. & Bon, J. (2013). Modelling drying kinetics of thyme (*Thymus vulgaris* L.): Theoretical and empirical models, and neural networks. *Food Sci. Technol. Int.*, 20, 13–22.
21. Sacilik, K. & Elicin, A.K. (2006). The thin layer drying characteristics of organic apple slices. *J. Food Eng.*, 73, 281–289.
22. Si, X., Wu, X., Yi, J.Y., Li, Z., Chen, Q., Bi, J. & Zhou, L. (2015). Comparison of different drying methods on the physical properties, bioactive compounds and antioxidant activity of raspberry powders. *J. Sci. Food Agric.*, 96, 2055–2062.
23. Siger, A., Antkowiak, W., Dwiecki, K., Rokosik, E., & Rudzińska, M. (2021). Nutlets of *Tilia cordata* Mill. and *Tilia platyphyllos* Scop.—Source of bioactive compounds. *Food Chemistry*, 346, 128888.
24. Singleton, V.L. & Rossi J.A. (1965). Colorimetry of total phenolics with phosphomolybdic-phosphotungstic acid reagents. *Am J Enol Viticult* 16:144–153.
25. Soysal, Y., Keskin, M., Arslan, A. & Sekerli, Y.E. (2018). Infrared drying characteristics of pepper at different maturity stages. *In Proceedings of the International Conference on Energy Research*, Alanya, Turkey, 1–2 November; pp. 293–304.
26. Tekin, Z.H. & Baslar, M. (2018). The effect of ultrasound-assisted vacuum drying on the drying rate and quality of red peppers. *J. Therm. Anal. Calorim.*, 132, 1131–1143.
27. Weryszko-Chmielewska, E. & Sadowska, D. A. (2010). The phenology of flowering and pollen release in four species of linden (*Tilia* L.). *Journal of Apicultural Science*, 54(2), 99-108.
28. Wissam, Z., Nour, A.A., Bushra, J., Zein, N. & Saleh, D. (2017). Extracting and studying the antioxidant capacity of polyphenols in dry linden leaves (*Tilia cordata*). *J. Pharmacogn. Phytochem.*, 6, 258–262.
29. Xiao, H., Pang, C., Wang, L., Bai, J., Yang, W. & Gao, Z. (2010). Drying kinetics and quality of Monukka seedless grapes dried in



- an air-impingement jet dryer. *Biosyst. Eng.*, 105, 233–240.
30. Yıldırım, A., Mavi, A., Oktay, M., Kara, A. A., Algur, Ö. F., & Bilaloğlu, V. (2000). Comparison of antioxidant and antimicrobial activities of Tilia (Tilia argentea Desf ex DC), sage (Salvia triloba L.), and Black tea (Camellia sinensis) extracts. *Journal of Agricultural and Food Chemistry*, 48(10), 5030-5034.

Corresponding author:

Ing. Kemal Çağatay Selvi, Ph.D., Department of Agricultural Machines and Technologies Engineering, Faculty of Agriculture, Ondokuz Mayıs University, Atakum 55139, Samsun, Turkey, phone: +90 507 9262829, e-mail: kcselvi74@gmail.com